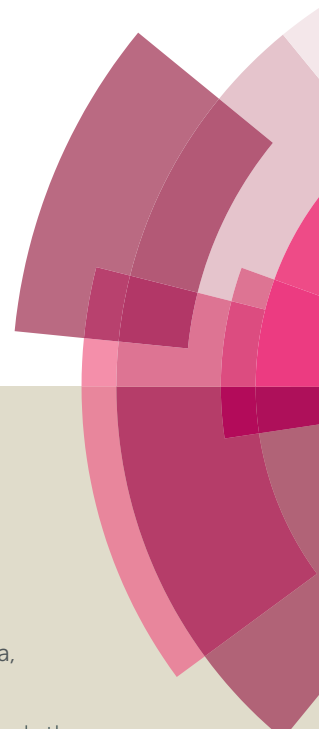


Organic & Biomolecular Chemistry

Accepted Manuscript



This article can be cited before page numbers have been issued, to do this please use: D. Kand, T. Saha, M. Lahiri and P. Talukdar, *Org. Biomol. Chem.*, 2015, DOI: 10.1039/C5OB00889A.



This is an *Accepted Manuscript*, which has been through the Royal Society of Chemistry peer review process and has been accepted for publication.

Accepted Manuscripts are published online shortly after acceptance, before technical editing, formatting and proof reading. Using this free service, authors can make their results available to the community, in citable form, before we publish the edited article. We will replace this *Accepted Manuscript* with the edited and formatted *Advance Article* as soon as it is available.

You can find more information about *Accepted Manuscripts* in the [Information for Authors](#).

Please note that technical editing may introduce minor changes to the text and/or graphics, which may alter content. The journal's standard [Terms & Conditions](#) and the [Ethical guidelines](#) still apply. In no event shall the Royal Society of Chemistry be held responsible for any errors or omissions in this *Accepted Manuscript* or any consequences arising from the use of any information it contains.



Journal Name

COMMUNICATION

Lysosome targeting fluorescence probe for imaging intracellular thiols

Received 00th January 20xx,
Accepted 00th January 20xxDnyaneshwar Kand,^{a†} Tanmoy Saha,^{a†} Mayurika Lahiri,^b and Pinaki Talukdar^{a*}

DOI: 10.1039/x0xx00000x

www.rsc.org/

A BODIPY-based fluorescence turn-on probe, exhibiting high selectivity and sensitivity towards intracellular thiols with excellent lysosomal localization is reported. Probe displayed fast response towards biothiols in aqueous solution. Localization of the probe in lysosome was demonstrated by intracellular colocalization studies with the aid of LysoSensor Green.

Cysteine (Cys), homocysteine (Hcy) and glutathione (GSH) are three important low molecular weight thiol biomolecules (biothiols) which perform various physiological functions essential for survival.¹ Alteration in intracellular and plasma levels of biothiols are associated with various diseases and disorders² *e.g.* abnormal levels of Cys results in hair depigmentation, edema, liver damage, slow growth in children etc.³ Hcy is known as a risk factor for cardiovascular and Alzheimer's diseases.⁴ GSH, a tripeptide is most abundant intracellular nonprotein thiol which plays a critical role in controlling oxidative stress in order to maintain the redox homeostasis,⁵ crucial for cell growth and function.⁶ Although, numerous fluorescent probes have been developed for selective detection of biothiols^{7–9} and cell imaging applications,^{7, 10–13} probes specific for locating in particular subcellular organelles are rare.^{14–26} Fluorescent probes for detection of biothiols in mitochondria are reported.^{27, 28}

Lysosome is an important cell organelle that contains approximately 50 different degradative enzymes which are active at the acidic pH (pH = 4–6) of the compartment.²⁹ The lysosomal membrane constitutes a physiological barrier between the lysosome matrix and the surrounding cytoplasm. The membrane's impermeability ensures the retention of both the lysosomal enzymes and their substrates within the lysosomes.³⁰ It is believed that GSH may be involved in stabilizing lysosome membranes.³¹ Thiols facilitate intralysosomal proteolysis by reducing disulphide bonds.³² For example, Cys is an effective stimulator of albumin degradation in liver lysosomes.³¹ For better understanding of the role of

lysosomal thiols it is important to develop thiol selective fluorescent probes capable of targeting lysosomes.

Herein, the design, synthesis and biothiol sensing properties of lysosome targeting fluorescence turn-on probe **1** are reported (Fig. 1). To obtain a photostable water soluble fluorescent thiol probe with excitation and emission wavelengths in the visible region boron-dipyrromethene (BODIPY) was selected as the fluorophore.³³ The necessary molecular decorations for thiol recognition and lysosome targeting were incorporated via 2,4-dinitrobenzenesulfonyl (DNs) group and morpholine ring,³⁴ respectively. As BODIPY-based chemosensors operate by perturbing the reduction potential of the *meso*-substituent,³⁵ the DNs group was attached to aryl group at *meso*-position.³⁶ Moreover, a phenyl ring at 5-position provided extended conjugation resulting in excitation at longer wavelengths while maintaining high quantum yield.³⁷

Synthesis of probe **1** was carried out from salicylaldehyde in five steps (Scheme 1). Dipyrromethane **3** was synthesized from salicylaldehyde **2** and pyrrole in presence of catalytic CF₃COOH in 64% yield. Compound **3** was dibrominated with two equivalents of *N*-bromosuccinimide in tetrahydrofuran at -78 °C and oxidized with DDQ in dichloromethane followed by addition of BF₃·Et₂O and Et₃N afforded the dibromo-BODIPY **4** in 60% yield. Reaction of **4** with morpholine resulted in BODIPY derivative **5** in 80% yield which on subsequent Suzuki coupling reaction with phenyl boronic acid provided compound **6** in 79% yield. Compound **6** upon treatment with 2,4-dinitrobenzenesulfonyl chloride provided probe **1** in 91% yield. Apart from the spectroscopic characterization of all compounds, single crystal X-ray diffraction structures for compound **5** and probe **1** were also recorded. Crystal structure analysis of probe

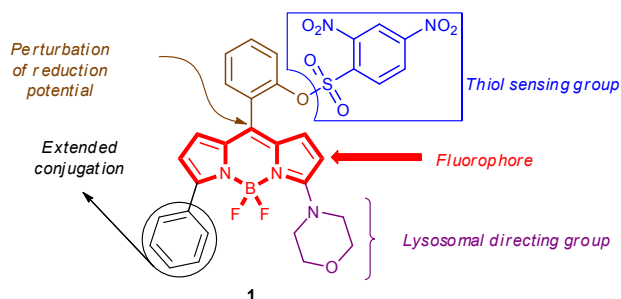


Fig. 1 Structure of the lysosomal targeting thiol probe **1**.

^a Department of Chemistry, Indian Institute of Science Education and Research Pune, Pune 411008, India. Email: ptalukdar@iiserpune.ac.in

^b Department of Biology, Indian Institute of Science Education and Research Pune, Pune 411008, India.

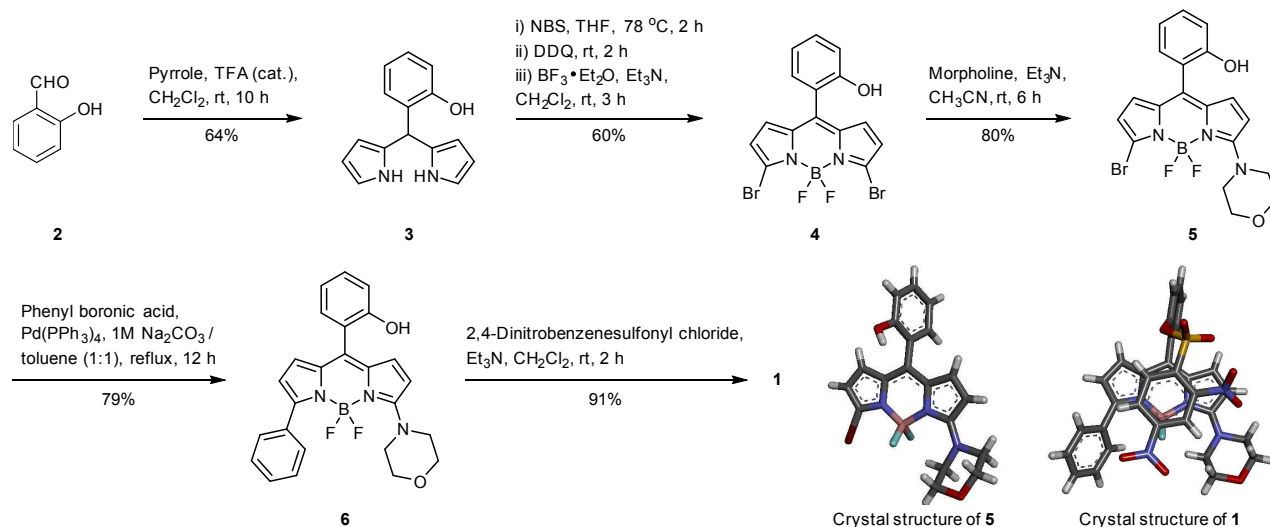
† D.K. and T.S. contributed equally to this work.

Electronic Supplementary Information (ESI) available: Experimental procedures, crystal structure parameters, analytical and spectroscopic data. See DOI: 10.1039/x0xx00000x



Journal Name

COMMUNICATION

Scheme 1 Synthesis of probe 1.^a

1 was useful to confirm the relative spatial arrangement between BODIPY and DN's moieties (Fig. S2).

To validate the fluorescence turn-on nature of sensing, the photophysical properties of compounds **1** and **6** were investigated in aqueous HEPES buffer (10 mM, pH 7.4, 1 mM CTAB) solution. The absorption spectrum of probe **1** exhibited $\lambda_{\text{max}} = 510$ nm with a molar extinction coefficient $\epsilon = 18600 \text{ M}^{-1} \text{ cm}^{-1}$ (see Fig. S3). The probe displayed very weak fluorescence ($\lambda_{\text{ex}} = 510$ nm) and quantum yield, $\Phi = 0.0026$ (standard: Rhodamine G, $\Phi = 0.76$ in water).³⁸ Compound **6** exhibited an absorption band centred at $\lambda_{\text{max}} = 515$ nm with a molar extinction coefficient $\epsilon = 23966 \text{ M}^{-1} \text{ cm}^{-1}$. The fluorescence spectrum acquired for **6** indicate a strong fluorescence emission centred at $\lambda_{\text{em}} = 584$ nm ($\lambda_{\text{ex}} = 510$ nm) and $\Phi = 0.17$ (standard: Rhodamine G, $\Phi = 0.76$ in water). This photophysical data satisfy the criteria of probe **1** to act as an efficient fluorescent turn-on probe. Reactivity of the probe **1** (10 μM) towards *n*-BuNH₂, Cys, GSH and Hcy (100 μM) were determined by fluorescence emission kinetics in HEPES buffer (10 mM, 1 mM CTAB, pH = 7.4). In each experiment, emission intensity at $\lambda = 585$ nm ($\lambda_{\text{ex}} = 510$ nm) was recorded with time (Fig. 2A). Addition of *n*-BuNH₂ to probe **1** did not indicate formation of fluorescent species during the reaction. A pronounced fluorescent intensity increase up to ~64-fold was obtained within 1 min after the addition of Cys ($t_{1/2} = 6.4$ s and pseudo first order rate constant, $k = 0.108 \text{ s}^{-1}$), Hcy ($t_{1/2} = 14.49$ s and $k = 0.0478 \text{ s}^{-1}$) and GSH ($t_{1/2} = 7.47$ s and $k = 0.0928 \text{ s}^{-1}$).

Quantitative turn-on response of probe **1** towards Cys was examined by fluorometric titrations. Sharp enhancements in fluorescence intensity (at $\lambda_{\text{em}} = 585$ nm) were observed (Fig. 2B) when titrations were carried out by addition of increasing

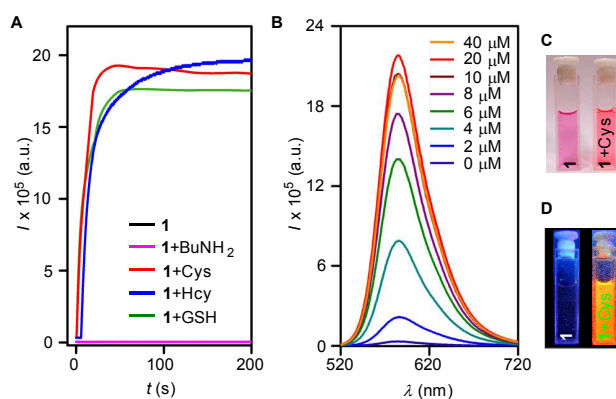


Fig. 2 (A) Fluorescence kinetics of probe **1** (10 μM) in 10 mM HEPES buffer, 1 mM CTAB, pH = 7.4) with various analytes (100 μM). All data were recorded at $\lambda_{\text{em}} = 585$ nm ($\lambda_{\text{ex}} = 510$ nm). (B) Fluorescence spectra of **1** (10 μM) in presence of Cys (0 to 40 μM) with $\lambda_{\text{ex}} = 510$ nm. Changes in visible color (C) and fluorescence (D) for **1** (10 μM) upon addition of Cys (100 μM).

concentrations of Cys (0, 2, 4, 6, 8, 10, 20 and 40 μM) to the probe **1** (10 μM) in HEPES buffer (10 mM, 1 mM CTAB, pH = 7.4). An equilibration time of 1 min was given after each addition of Cys to ensure the completion of reaction. When fluorescence intensities at 585 nm were plotted against concentrations of Cys, good linear correlation (Regression factor, $R = 0.9686$) was observed up to one equivalent of the Cys added (Fig. S6A). A detection limit of 8.2 nM was calculated for the probe **1**, based on signal to noise ratio, $S/N = 3$. Sensing of Cys by **1** was also associated with the change in color

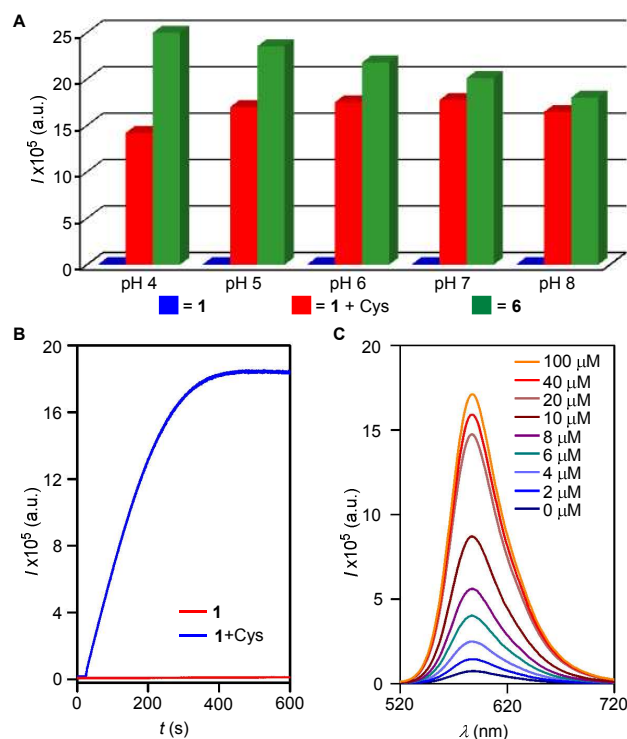


Fig. 3 Fluorescence intensities at 585 nm for probe **1** (blue), probe **1**+Cys (red) and compound **6** (green) at pH 4, 5, 6, 7 and 8, respectively in phosphate buffer (10 mM, 1 mM CTAB) (A). Fluorescence kinetics measurements of probe **1** (10 μ M) with and without addition of Cys (100 μ M) recorded at 585 nm (λ_{ex} = 510 nm) in phosphate buffer (10 mM, 1 mM CTAB, pH = 5) (B). Fluorescence spectra of **1** (10 μ M) in presence of Cys (0 to 100 μ M) with λ_{ex} = 510 nm in phosphate buffer (10 mM, 1 mM CTAB, pH = 5) (C).

from orchid to hot pink under the ambient light (Fig. 2C) and excitation under hand held UV-lamp (λ_{ex} = 365 nm) resulted in the appearance of orange fluorescence (Fig. 2D).

We have already stated that the lysosomal pH ranges between 4–6.³⁹ As a lysosome targeting probe for biothiols, the molecule should also respond to biothiols in the pH range of lysosome. To verify this, fluorescence intensities (at 585 nm) of probe **1** (10 μ M) and compound **6** (10 μ M) were individually recorded in phosphate buffer (10 mM, 1 mM CTAB) at pH values 4, 5, 6, 7 and 8 (Fig. 3A). Simultaneously the sensing activity of **1** (10 μ M) was monitored at pH = 4–8 by treating with Cys (100 μ M) in phosphate buffer (10 mM, 1 mM CTAB) for 10 min. From this study, response of the probe towards Cys at pH lower than the physiological pH was observed, and fluorescence enhancements in the pH range of 4–8 were also comparable. Encouraged by this results, reactivity of the probe **1** (10 μ M) towards Cys (100 μ M) at pH 5 was monitored in phosphate buffer (10 mM, 1 mM CTAB, pH = 5). For free probe, no fluorescence intensity enhancement λ = 585 nm (λ_{ex} = 510 nm) was observed indicating the stability of the compound under acidic pH (Fig. 3B). However, a sharp enhancement of fluorescent intensity up to ~95-fold was obtained within 8 min after the addition of Cys. From this reaction kinetics, k = 0.00553 s⁻¹ and $t_{1/2}$ = 125.3 s were calculated. The slower rate in comparison with pH 7.4 can be rationalized with the lower nucleophilicity of the thiol group of Cys. Moreover, quantitative turn-on response of probe **1** towards Cys in phosphate buffer (10 mM, 1 mM CTAB, pH = 5) was also examined

by fluorometric titrations. Significant enhancements in fluorescence intensity (at λ_{em} = 585 nm) were observed when titrations were carried out by adding increasing concentrations of Cys (0, 2, 4, 6, 8, 10, 20, 40 and 100 μ M) in the probe **1** (10 μ M) at this pH (Fig. 3C). An equilibration time of 8 min was given after each addition of Cys to ensure the completion of reaction. When fluorescence intensities at 585 nm were plotted against concentrations of Cys, a linear correlation (Regression factor, R^2 = 0.9787) was observed up to one equivalent of the Cys added (Fig. S6B). A detection limit of 95.7 nM was calculated for the probe **1**, based on signal to noise ratio, S/N = 3.

To prove the formation of compound **6** during the thiol sensing, HPLC studies were carried out under a gradient method using CH₃CN and H₂O eluent (for details information see SI). HPLC chromatograph of pure probe **1** provided the retention time, t_R = 17.56 min while, t_R = 16.34 min was obtained for compound **6** (Fig. 4). Compound **1** upon treatment with Cys (0.5 and 1.0 equiv) clearly showed consumption of the probe and formation of **6** (Fig. 4). MALDI-TOF analysis of the isolated compound corresponding to t_R = 16.34 min showed m/z = 445.13 confirming the formation of compound **6** (Fig. S9).

In next stage, the selectivity of probe **1** towards biological thiols

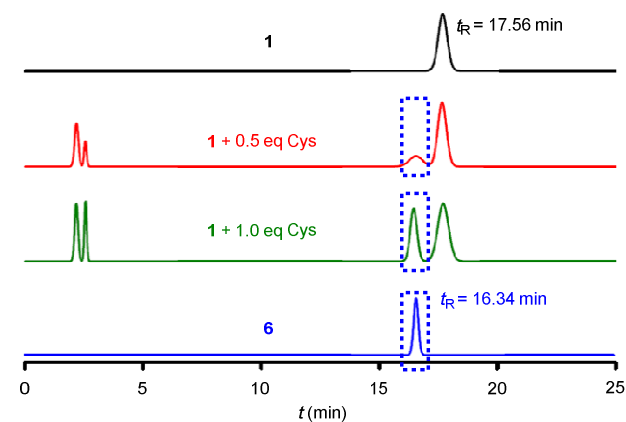


Fig. 4 HPLC chromatograms of probe **1** (10 μ M) upon reaction with Cys (0.5 and 1.0 equivalent) recorded in a gradient solvent system of CH₃CN and H₂O.

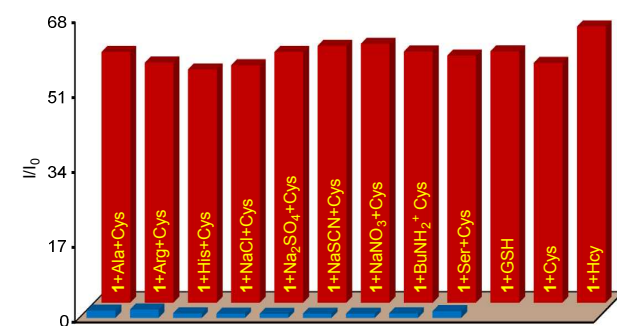


Fig. 5 Relative fluorescence intensity enhancements (I/I_0) at 585 nm for probe **1** (10 μ M) towards Ala, Arg, His, NaCl, Na₂SO₄, NaSCN, NaNO₃, BuNH₂, Ser, GSH, Cys and Hcy (100 μ M each) in HEPES buffer. Front row: changes in intensities in the presence of non-thiol based analytes (100 μ M); First nine bars of back row: changes in intensities upon addition of Cys (100 μ M) to the resulting solutions of non-thiol addition. Last three bars of back row: changes in intensities upon addition of GSH, Cys and Hcy (100 μ M each) to probe **1** (10 μ M).

COMMUNICATION

was examined under physiological pH. In each case, probe **1** (10 μM) was treated separately with 100 μM of each analyte (either of Ala, Arg, His, NaCl, Na_2SO_4 , NaSCN, NaNO_3 , BuNH_2 , Ser, GSH, Cys and Hcy) in HEPES buffer (10 mM, 1 mM CTAB, pH = 7.4) and fluorescence spectra (λ_{ex} = 510 nm) were recorded after 5 minutes at room temperature. No significant fluorescence enhancement was observed for analytes non-thiol analytes (Fig. 5). Treatment of probe **1** with GSH, Cys and Hcy under identical conditions provided strong fluorescence enhancements in the range of 54 – 63 fold. Comparable fluorescence enhancements were observed upon addition of Cys to the solutions pre-treated with non-thiol analytes. This study demonstrates the effectiveness of compound **1** as a selective probe for biothiols under competitive environments.

Based on the aforesaid outcome, localization of probe **1** in the lysosome and its ability to sense biological thiols in living cells were examined. First, the cell permeability and intracellular thiol sensing ability of probe **1** was evaluated by live-cell imaging of Human cervical cancer cell line (HeLa). Strong fluorescence was observed when HeLa cells were incubated with probe **1** (10 μM in 1:100 DMSO-DNEM v/v, pH = 7.4) at 37 $^\circ\text{C}$ for 10 min (Fig. 6B and E). These cells then incubated with commercially available lysosome specific dye-LysoSensor Green (1.0 μM) showed green fluorescence (Fig. 6D). Colocalization image of green and red channels shows the localization of probe **1** in lysosomes (Fig. 6F). In control experiment, cells were pre-treated with an excess (5 mM) of the thiol-reactive *N*-phenylmaleimide and then incubated with the probe **1**. The confocal microscopic studies did not show fluorescence signal (Fig. 6C). This confirms the specificity of probe **1** for thiols over other analytes in living cells.

Next, the colocalization experiments were performed by co-staining HeLa cells with LysoSensor Green and probe **1** to determine the location of fluorescence emission. When HeLa cells were incubated with probe **1** (5 μM in 1:100 DMSO-DNEM v/v, pH = 7.4) at 37 $^\circ\text{C}$ for 10 min, strong red fluorescence was observed (Fig. 7A). These cells were then incubated with LysoSensor Green (1 μM in 1:100 DMSO-DNEM v/v, pH = 7.4) at 37 $^\circ\text{C}$ for 10 min showed green fluorescence (Fig. 7B). As seen in Fig. 7C the fluorescence image of probe **1** was mainly overlapped with that of LysoSensor Green indicates ability of probe **1** to target lysosomes. The intensity profiles of the linear regions of interest (ROI) across HeLa cells stained with probe **1** and LysoSensor Green vary in close synchrony (Fig. 7D). Pearson's coefficient and overlap coefficient are 0.963 and 0.984, respectively; evaluated using the conventional dye overlay method. Overlap coefficients k_1 and k_2 found to be 0.9 and 1.1 respectively. Colocalization coefficients (Manders' Coefficients) $M_1 = 0.77$ (fraction of LysoSensor Green overlapping probe) and $M_2 = 0.818$ (fraction of probe overlapping LysoSensor Green) also confirms an excellent overlap. An intensity correlation analysis (ICA) is employed to assess the intensity distribution of the two co-existing dyes. The pixel intensity of the LysoSensor Green was plotted against that of the probe **1** (Fig. 7E). The dependent staining results in a highly correlated plot, and the ICA plots for the two stains generate an unsymmetrical hourglass-shaped scatter plot that are markedly skewed toward positive values (Fig. 7F, G). Li's intensity correlation quotient (ICQ) for the two dyes is 0.459, very close to 0.5, suggesting that the staining intensities are dependent on each other.

The cytotoxicity of probe **1** was determined by MTT assay.

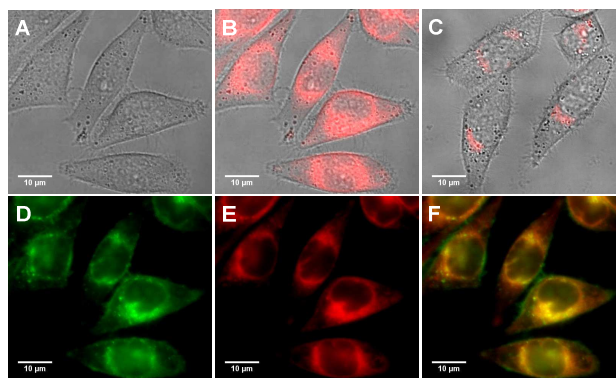


Fig. 6 DIC image (A), overlay of fluorescence and DIC images (B), of HeLa cells incubated with of probe **1** (5.0 μM) for 10 min. Overlay image of fluorescence and DIC of cells pre-incubated with *N*-phenylmaleimide (5 mM) for 30 min followed by incubation with probe **1** (5 μM) for 10 min (C). Fluorescence image of cells pre-incubated with probe **1** (5.0 μM) for 10 min followed by incubation with LysoSensor Green (1.0 μM) for 10 min, green channel (D), red channel (E) and overlay image of images D and E. (F).

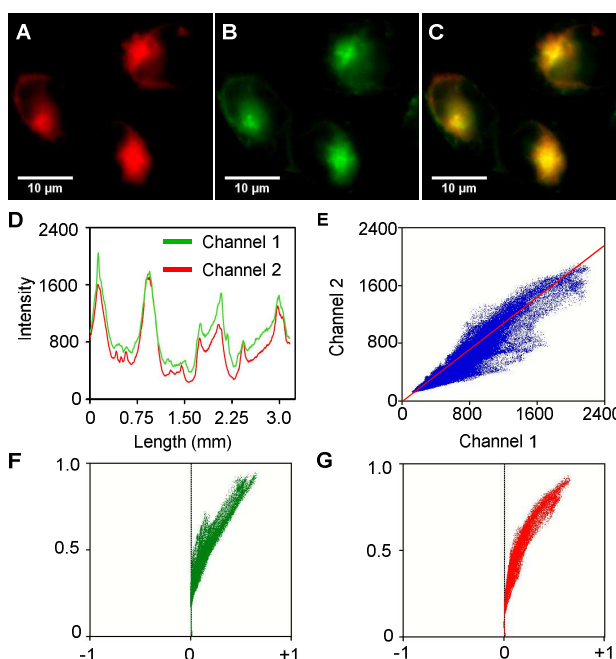


Fig. 7 Colocalization experiments using probe **1** to lysosomes in HeLa cells. HeLa cells were stained with (A) probe **1** (5.0 μM) for 5 min at 37 $^\circ\text{C}$ and (B) LysoSensor Green (1.0 μM) (C) Overlay of (A) and (B). (D) Intensity profile of regions of interest (ROI) across HeLa cells. (E) Intensity correlation plot of stain probe **1** and LysoSensor Green. ICA plots of (F) stain LysoSensor Green and (G) probe **1**.

Various concentrations of probe **1** (5, 10, 20 and 50 μM) were used to determine toxicity level of probe towards HeLa cell. The result revealed that cells were not affected by incubation with probe **1** (up to 10 μM) for 2 h as about 95% cell viability was determined at 10 μM concentration of probe **1** (Fig. S8).

Conclusions

In summary, we have developed lysosome targeting BODIPY-based fluorescence turn-on probe for rapid, selective and sensitive detection of biothiols. At pH 7.4, the probe displayed very fast

reaction with biothiols such as Cys, Hcy and GSH. Reaction of the probe with Cys provided pseudo first order rate constant, $k = 0.108 \text{ s}^{-1}$ and $t_{1/2} = 6.4 \text{ s}$. The reaction also provided ~ 64 -fold fluorescence enhancement within 1 min of reaction. The probe was also reactive towards the biothiol at pH 5 however, with lower value of $k = 0.00553 \text{ s}^{-1}$ and longer $t_{1/2} = 125.3 \text{ s}$. At this pH, a sharp enhancement of fluorescent intensity up to ~ 95 -fold was obtained after 8 min of Cys addition. Live-cell imaging studies of HeLa cells confirmed the cell permeability, lysosome specificity and intracellular biothiol detection ability of the probe. MTT assay disclosed about 95% cell viability at $10 \text{ }\mu\text{M}$ concentration of the probe.

Acknowledgements

We acknowledge IISER Pune and DST-SERB (Grant No. SR/S1/OC-65/2012) for financial supports. D.K. thanks CSIR, and T.S. thanks UGC for research fellowships.

Notes and references

1. S. Zhang, C.-N. Ong and H.-M. Shen, *Cancer Lett.*, 2004, **208**, 143-153.
2. J. Nourooz-Zadeh, *Biothiols in Health and Disease*, editors: Lester Packer and Enrique Cadenas, 1996.
3. S. Shahrokhian, *Anal. Chem.*, 2001, **73**, 5972-5978.
4. H. Refsum, P. M. Ueland, O. Nygard and S. E. Vollset, *Annu. Rev. Med.*, 1998, **49**, 31-62.
5. Z. A. Wood, E. Schroder, J. Robin Harris and L. B. Poole, *Trends Biochem. Sci.*, 2003, **28**, 32-40.
6. T. P. Dalton, H. G. Shertzer and A. Puga, *Annu. Rev. Pharmacol. Toxicol.*, 1999, **39**, 67-101.
7. H. S. Jung, X. Chen, J. S. Kim and J. Yoon, *Chem. Soc. Rev.*, 2013, **42**, 6019-6031.
8. S. Sreejith, K. P. Divya and A. Ajayaghosh, *Angew. Chem., Int. Ed.*, 2008, **47**, 7883-7887.
9. X. Zhang, X. Ren, Q.-H. Xu, K. P. Loh and Z.-K. Chen, *Org. Lett.*, 2009, **11**, 1257-1260.
10. X. Chen, Y. Zhou, X. Peng and J. Yoon, *Chem. Soc. Rev.*, 2010, **39**, 2120-2135.
11. L.-L. Yin, Z.-Z. Chen, L.-L. Tong, K.-H. Xu and B. Tang, *Fenxi Huaxue*, 2009, **37**, 1073-1081.
12. L. Zhu, Z. Yuan, J. T. Simmons and K. Sreenath, *RSC Adv.*, 2014, **4**, 20398-20440.
13. H. Li, J. Fan and X. Peng, *Chem. Soc. Rev.*, 2013, **42**, 7943-7962.
14. X. Chen, S.-K. Ko, M. J. Kim, I. Shin and J. Yoon, *Chem. Commun.*, 2010, **46**, 2751-2753.
15. D. Kand, A. M. Kalle, S. J. Varma and P. Talukdar, *Chem. Commun.*, 2012, **48**, 2722-2724.
16. W. Lin, L. Long and W. Tan, *Chem. Commun.*, 2010, **46**, 1503-1505.
17. Y.-Q. Sun, M. Chen, J. Liu, X. Lv, J.-f. Li and W. Guo, *Chem. Commun.*, 2011, **47**, 11029-11031.
18. B. Tang, L. Yin, X. Wang, Z. Chen, L. Tong and K. Xu, *Chem. Commun.*, 2009, 5293-5295.
19. M. Zhang, M. Yu, F. Li, M. Zhu, M. Li, Y. Gao, L. Li, Z. Liu, J. Zhang, D. Zhang, T. Yi and C. Huang, *J. Am. Chem. Soc.*, 2007, **129**, 10322-10323.
20. J. Bouffard, Y. Kim, T. M. Swager, R. Weissleder and S. A. Hilderbrand, *Org. Lett.*, 2008, **10**, 37-40.
21. W. Sun, W. Li, J. Li, J. Zhang, L. Du and M. Li, *Tetrahedron Lett.*, 2012, **53**, 2332-2335.
22. D. Kand, A. M. Kalle and P. Talukdar, *Org. Biomol. Chem.*, 2013, **11**, 1691-1701.
23. B. Zhu, X. Zhang, Y. Li, P. Wang, H. Zhang and X. Zhuang, *Chem. Commun.*, 2010, **46**, 5710-5712.
24. J. Shao, H. Sun, H. Guo, S. Ji, J. Zhao, W. Wu, X. Yuan, C. Zhang and T. D. James, *Chem. Sci.*, 2012, **3**, 1049-1061.
25. K. Sreenath, Z. Yuan, J. R. Allen, M. W. Davidson and L. Zhu, *Chem. Eur. J.*, 2015, **21**, 867-874.
26. D. Kim, G. Kim, S.-J. Nam, J. Yin and J. Yoon, *Sci. Rep.*, 2015, **5**, 1-8.
27. S. Singha, D. Kim, A. S. Rao, T. Wang, K. H. Kim, K.-H. Lee, K.-T. Kim and K. H. Ahn, *Dyes Pigments*, 2013, **99**, 308-315.
28. C. S. Lim, G. Masanta, H. J. Kim, J. H. Han, H. M. Kim and B. R. Cho, *J. Am. Chem. Soc.*, 2011, **133**, 11132-11135.
29. H. Zhu, J. Fan, Q. Xu, H. Li, J. Wang, P. Gao and X. Peng, *Chem. Commun.*, 2012, **48**, 11766-11768.
30. C. L. Andrew, A. R. Klemm and J. B. Lloyd, *Biochim. Biophys. Acta*, 1997, **1330**, 71-82.
31. J. L. Mego, *Biochemical J.*, 1984, **218**, 775-783.
32. B. Arunachalam, U. T. Phan, H. J. Geuze and P. Cresswell, *Proc. Nat. Acad. Sci.*, 2000, **97**, 745-750.
33. N. Boens, V. Leen and W. Dehaen, *Chem. Soc. Rev.*, 2012, **41**, 1130-1172.
34. T. Liu, Z. Xu, D. R. Spring and J. Cui, *Org. Lett.*, 2013, **15**, 2310-2313.
35. A. Loudet and K. Burgess, *Chem. Rev.*, 2007, **107**, 4891-4932.
36. H. Guo, Y. Jing, X. Yuan, S. Ji, J. Zhao, X. Li and Y. Kan, *Org. Biomol. Chem.*, 2011, **9**, 3844-3853.
37. C. Thivierge, R. Bandichhor and K. Burgess, *Org. Lett.*, 2007, **9**, 2135-2138.
38. J. Olmsted, III, *J. Phys. Chem.*, 1979, **83**, 2581-2584.
39. K. A. Christensen, J. T. Myers and J. A. Swanson, *J. Cell Sci.*, 2002, **115**, 599-607.